17

Diffraction from Small Volumes

CHAPTER PREVIEW

A very important concept in TEM is that we only ever diffract from small volumes. These volumes are now called nanoparticles, nanograins, nanobelts, etc. By definition, no TEM specimen is infinite in all directions and all defects are small. Of course, the beam is also never infinitely wide! This chapter therefore discusses how the size of what we are examining influences the appearance of the DP. Although we will discuss many different aspects of diffraction, there are three important ideas that underlie all this discussion

- We are diffracting from small volumes.
- We are diffracting from crystals.
- We need to index the DPs we see and relate the patterns to the image.

The fact that it is possible to obtain diffraction from several planes in a zone at the same time is due to the effect of the specimen shape on the diffracted-intensity distribution. The diffraction spot is only a mathematical point if the specimen is perfect and infinite in all directions. For example, a TEM specimen is effectively infinite ($\sim$3 mm) relative to the unit-cell dimensions in the plane of the specimen, but very thin ($< 0.5\,\mu$m) parallel to the electron beam. This means that the diffracted intensity can be represented in the reciprocal lattice as a relrod (see Chapter 12) stretched parallel to the electron beam in reciprocal space, rather than as a point, and the relrod does have a width. Therefore, over a range of angles, the Ewald sphere will still intercept the relrod and diffracted intensity will still be generated. This is equivalent to saying that the Laue condition is relaxed in one dimension in the TEM owing to the specimen shape. For this reason, accurate structural analysis of unknown specimens is very difficult in conventional TEM diffraction, and X-rays are usually the most accurate method for structure determination if your specimen is large. However, we will reconsider this statement in Chapter 21.

17.1 INTRODUCTION

In Chapter 12, we stated that each point in the reciprocal lattice can actually be associated with a rod. This construction allowed us to discuss the geometry of DPs, taking account of the experimental fact that we see spots in the DP even when **s** is not exactly zero. In fact, without this construction, there is no reason to discuss **s**. Now we are going to show quantitatively why we have rods. As we suggested earlier, the reason is that we have a thin specimen: a small thickness in real space gives a large length in reciprocal space. This concept is valid in all directions, not just parallel to the electron beam. Hence, we call this the 'shape effect.' The intensity in the diffracted beam is strongest for a given thickness when $\mathbf{K} = \mathbf{g}$, but we still have intensity when **K** is not exactly equal to **g**, or when

$$\mathbf{K} = \mathbf{g} + \mathbf{s} \tag{17.1}$$

Then we can write, from equation 13.48

$$\left|\phi_{\mathbf{g}}\right|^2 = \left(\frac{\pi t}{\xi_{\mathbf{g}}}\right)^2 \cdot \frac{\sin^2(\pi t s_{\text{eff}})}{(\pi t s_{\text{eff}})^2} \tag{17.2}$$

We model the specimen as a thin rectangular slab as shown in Figure 17.1. To keep the math simple, we will assume that we have a rectangular unit cell with sides a, b, c and that there are N_x cells in the x direction, N_y in

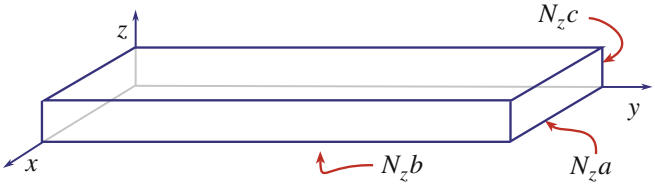

FIGURE 17.1. An idealized thin-foil specimen modeled as a rectangular slab made up of rectangular unit cells of sides *a, b, c*. There are N_x cells in the *x* direction, N_y in the *y* direction and N_z in the *z* direction.

the *y* direction and N_z in the *z* direction. All that we have to do to determine the total diffracted amplitude is to add the amplitudes from each cell, allowing for the phase factor that is present, because the cells are displaced from one another. Each cell has the same structure factor *F*.

We can do the addition of amplitudes in two ways. The first way is to do the summation. In the second, we will show how the same result follows if you start with the integral expression for $\phi_{\mathbf{g}}$. These expressions lead to the important idea of a relrod and subsidiary maxima; in DPs we can see the effects of the relrods, but you may never see the subsidiary maxima.

What we are going to do is derive equations for the shape of the relrods which were introduced in Section 12.5 and which we used in Chapter 13 to explain why we 'see' spots in the DP even when $\mathbf{s} \neq 0$. This whole approach gives us a pictorial aid to understanding diffraction from small volumes. After developing the theory for the simple case, we will go on to discuss the complications introduced because we look at real materials, and specimens of real materials are usually not flat platelets.

17.1.A The Summation Approach

This approach starts with expressing the total amplitude, *A*, of the diffracted beam as the sum of contributions from all the individual cells in a parallel-sided specimen. (Note: this is a kinematical approach and ignores dynamical scattering.)

$$A = F\sum_{n_x} e^{\mathrm{i}\,2\pi n_x \mathbf{K}.\mathbf{a}} \sum_{n_y} e^{\mathrm{i}\,2\pi n_y \mathbf{K}.\mathbf{b}} \sum_{n_z} e^{\mathrm{i}\,2\pi n_z \mathbf{K}.\mathbf{c}} \tag{17.3}$$

Here n_x, n_y and n_z have their usual meanings and all are integers; we have $N_x \times N_y \times N_z$ cells in the specimen. As shown in Figure 17.1, we will let n_x vary from 0 to N_x–1 and similarly with n_y and n_z. The location of each unit cell is then defined by the vector $\mathbf{r}_n$

$$\mathbf{r}_n = n_x\mathbf{a} + n_y\mathbf{b} + n_z\mathbf{c} \tag{17.4}$$

To simplify the first summation we set *X* equal to $e^{\mathrm{i}2\pi\mathbf{K}.\mathbf{a}}$. Then each separate summation term is a geometric series, so we can sum the n_x series as

$$\begin{gathered} S = \sum_{n_x=0}^{n_x=N_x-1} X^n = X^0 + X^1 + \ldots X^{N_x-1} \\ SX = X^1 + X^2 + \ldots X^{N_x} = X^{N_x} - X^0 + S \\ S = \frac{1 - X^{N_x}}{1 - X} \end{gathered} \tag{17.5}$$

Now replace *X* by $e^{\mathrm{i}2\pi\mathbf{K}.\mathbf{a}}$ to find the sum.

$$\sum_{n_x=0}^{n_x=N_x-1} e^{\mathrm{i}\,2\pi n_x \mathbf{K}.\mathbf{a}} = \frac{1 - e^{\mathrm{i}\,2\pi N_x \mathbf{K}.\mathbf{a}}}{1 - e^{\mathrm{i}\,2\pi \mathbf{K}.\mathbf{a}}} \tag{17.6}$$

Since we are interested in the intensities, we multiply this sum by its complex conjugate. To do this we use some simple trigonometric relationships

$$\begin{aligned} \left(1-e^{-\mathrm{i}\alpha}\right)\left(1-e^{\mathrm{i}\alpha}\right) &= (1-\cos\alpha+\mathrm{i}\sin\alpha)(1-\cos\alpha-\mathrm{i}\sin\alpha) \\ &= \left(1-2\cos\alpha+\cos^2\alpha\right)+\sin^2\alpha = 2(1-\cos\alpha) = 4\sin^2\frac{\alpha}{2} \end{aligned} \tag{17.7a}$$

or

$$\left(1 - e^{-\mathrm{i}\,\alpha}\right)\left(1 - e^{\mathrm{i}\,\alpha}\right) = 4\left(\frac{e^{\mathrm{i}\frac{\alpha}{2}} - e^{-\mathrm{i}\frac{\alpha}{2}}}{2}\right)\left(\frac{e^{-\mathrm{i}\frac{\alpha}{2}} - e^{\mathrm{i}\frac{\alpha}{2}}}{2}\right) \tag{17.7b}$$

The intensity is then related to

$$\left|\sum_{n_x=0}^{n_x=N_x-1} e^{\mathrm{i}2\pi n_x \mathbf{K}.\mathbf{a}}\right|^2 = \frac{\left(1 - e^{-\mathrm{i}2\pi N_x \mathbf{K}.\mathbf{a}}\right)}{1 - e^{-\mathrm{i}2\pi \mathbf{K}.\mathbf{a}}} \frac{\left(1 - e^{-\mathrm{i}2\pi N_x \mathbf{K}.\mathbf{a}}\right)}{1 - e^{-\mathrm{i}2\pi \mathbf{K}.\mathbf{a}}} \tag{17.8a}$$

or

$$\left|\sum_{n_x=0}^{n_x=N-1} e^{\mathrm{i}2\pi N_x \mathbf{K}.\mathbf{a}}\right|^2 = \frac{4\sin^2(\pi N_x \mathbf{K}.\mathbf{a})}{4\sin^2(\pi \mathbf{K}.\mathbf{a})} \tag{17.8b}$$

Then we can write

$$\begin{aligned} I = |A|^2 = |F|^2 &\left(\frac{\sin^2(\pi N_x \mathbf{K}.\mathbf{a})}{\sin^2(\pi \mathbf{K}.\mathbf{a})}\right) \\ &\left(\frac{\sin^2(\pi N_y \mathbf{K}.\mathbf{b})}{\sin^2(\pi \mathbf{K}.\mathbf{b})}\right)\left(\frac{\sin^2(\pi N_z \mathbf{K}.\mathbf{c})}{\sin^2(\pi \mathbf{K}.\mathbf{c})}\right) \end{aligned} \tag{17.9}$$

If the dot product $\mathbf{K}.\mathbf{a}$ is an integer, then the first of these terms is unity. This is, of course, the Bragg condition and the intensity is then a maximum. There are also subsidiary maxima or minima when

$$\pi N_x \mathbf{K}.\mathbf{a} = \frac{\pi}{2} C \tag{17.10}$$

where C = an integer. Reordering this equation, we have

$$\mathbf{K}.\mathbf{a} = \frac{C}{2N_x} \tag{17.11}$$

Equation 17.9 is the basis of the shape effect and leads to the idea of the relrod, which you recall is the name we give to a reciprocal-lattice rod (look back at Section 12.5).

17.1.B The Integration Approach

If we take equation 13.2, which is the amplitude diffracted by a single unit cell, and sum this over all the cells in the specimen, the amplitude of the diffracted beam can be written as

$$\phi_{\mathbf{g}} = \frac{e^{2\pi i \mathbf{k}.\mathbf{r}}}{r} \sum_n F_n e^{(-2\pi i \mathbf{K}.\mathbf{r}_n)} \qquad (17.12)$$

Since we have defined **K** to be **g** + **s**, we can rewrite this equation as

$$\phi_{\mathbf{g}} = \frac{e^{2\pi i \mathbf{k}.\mathbf{r}}}{r} \sum_n F_{\mathbf{g}} e^{\left(-2\pi i (\mathbf{g}+\mathbf{s}_{\mathbf{g}}).\mathbf{r}_n\right)} \qquad (17.13)$$

Now we know that $\mathbf{g}.\mathbf{r}_n$ is an integer by the definition of **g** and $\mathbf{r}_n$ and we will refer to $\mathbf{s}_{\mathbf{g}}$ as **s**. Hence we can write equation 17.13 as

$$\phi_{\mathbf{g}} = \frac{e^{2\pi i \mathbf{k}.\mathbf{r}}}{r} \sum_n F_{\mathbf{g}} e^{(-2\pi i \mathbf{s}.\mathbf{r}_n)} \qquad (17.14)$$

where **s** is the deviation parameter for reflection **g**. If we make the approximation that the crystal contains many unit cells, we can replace this sum by an integral to give

$$\phi_{\mathbf{g}} = \frac{e^{2\pi i \mathbf{k}.\mathbf{r}}}{rV_c} F_{\mathbf{g}} \int_{\text{crystal}} e^{(-2\pi i \mathbf{s}.\mathbf{r}_n)} dv \qquad (17.15)$$

This is where the present treatment differs from the first. If we now express **s** and $\mathbf{r}_n$ as the vectors

$$\mathbf{s} = u\mathbf{a}^* + v\mathbf{b}^* + w\mathbf{c}^* \qquad (17.16)$$

and

$$\mathbf{r}_n = h\mathbf{a} + k\mathbf{b} + l\mathbf{c} \qquad (17.17)$$

then we can write

$$\phi_{\mathbf{g}} = \frac{e^{2\pi i \mathbf{k}.\mathbf{r}}}{rV_c} F_{\mathbf{g}} \int_0^C \int_0^B \int_0^A e^{-2\pi i(ux+vy+wz)} dx dy dz \qquad (17.18)$$

where $A = N_x a$, etc. This integral is straightforward.

$$\int_0^A e^{-2\pi i u x} = \frac{e^{-2\pi i u A} - 1}{-2\pi i u} = \left(\frac{e^{-\pi i u A}}{\pi u}\right)\left(\frac{e^{\pi i u A} - e^{-\pi i u A}}{2i}\right)$$

$$= \frac{e^{-\pi i u A}}{\pi u} \sin(\pi u A) \qquad (17.19)$$

$$\phi_{\mathbf{g}} = \frac{e^{2\pi i \mathbf{k}.\mathbf{r}}}{rV_c} F_{\mathbf{g}} \frac{(\sin \pi A u)}{(\pi u)} \frac{(\sin \pi B v)}{(\pi v)} \frac{(\sin \pi C w)}{(\pi w)} e^{iD} \qquad (17.20)$$

(D is an unimportant phase factor.) The intensity is then as given by equation 17.9, but we have explicitly kept the r^{-2} and V_c^{-2} dependence for the intensities.

You should recognize the form of equations 17.9 and 17.20. These equations have the same form as that given back in equation 2.12 for diffraction from a diffraction grating. The corresponding diffraction grating has N_x lines which are spaced a distance a apart. The physical similarity is that the grating, just like our crystal, has a finite size.

17.2 THE THIN-FOIL EFFECT

Equation 17.9 is very important for TEM. It tells us why the relrods we introduced in Chapter 12 have a finite length if we measure them to the first minimum. It also tells us that the diffracted intensity does depend on the value of **s**; it is not a constant for any position along the rod.

RELRODS AND INTENSITY

Just remember that when we said "the intensity" we meant "the intensity which the diffracted beam will have if s takes a particular value; i.e., if the Ewald sphere cuts the relrod at that point."

We can better appreciate this variation along the rod if we plot the intensity and draw the Ewald sphere, as shown in Figure 17.2. We only draw the intensity plot for one direction at a time. This diagram shows the Ewald sphere cutting the relrod on one side while showing the intensity along the relrod on the right-hand plot.

Figure 17.2 is an extension of Ewald's 'pictorial representation' of diffraction. We can now draw the reciprocal lattice as shown for a simple-cubic crystal in Figure 17.3, such that every point is replaced by a relrod and every relrod is described by equation 17.9. If the surface of the crystal is exactly parallel to the (112) plane, but we orient the specimen slightly off the [001] pole, then the Ewald sphere cuts the relrod as different positions relative to the square array of spots, which is the projection of the spots at zero tilt (Figure 17.3B). The DP will appear as shown in Figure 17.3C. In Figure 17.3C, C is the projected position of the center of the

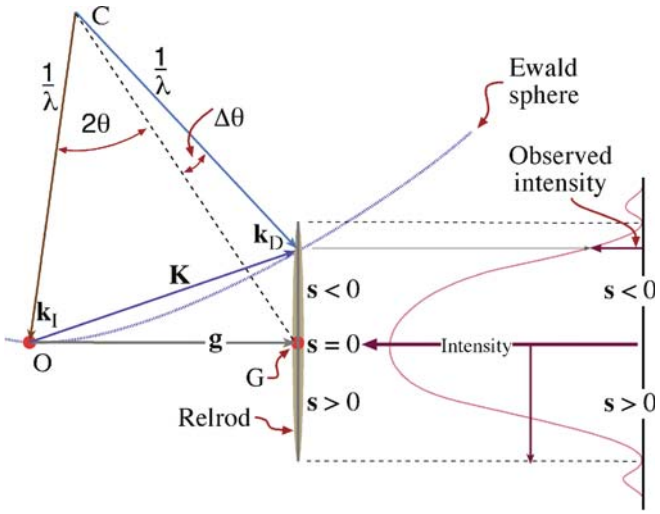

FIGURE 17.2. The relrod at $\mathbf{g}_{hkl}$ when the beam is $\Delta\theta$ away from the exact Bragg condition. The Ewald sphere intercepts the relrod at a negative value of **s** which defines the vector $\mathbf{K} = \mathbf{g} + \mathbf{s}$. The intensity of the diffracted beam as a function of where the Ewald sphere cuts the relrod is shown on the right of the diagram. In this case the intensity has fallen to almost zero.

Ewald sphere. As an exercise, consider whether the pattern would differ if the surface were cut slightly off (001) but oriented at the [001] pole. Then repeat the first exercise but instead of tilting the specimen, tilt the electron beam through the same small angle.

Remember that we deduced equation 17.9 by simply adding the amplitudes from all the unit cells, taking the position of the cells into account.

We calculated a 'structure factor' for the whole volume which contributes to $\phi_{\mathbf{g}}$: we call this calculated factor the shape factor.

We should then use this shape factor rather than the structure factor (since F is included in equation 17.9) in our dynamical calculations of $\phi_{\mathbf{g}}$. The problem is, of course, that the shape factor can be different for every specimen we examine.

We have just deduced a method for picturing how the shape of a perfect parallelepiped (of sides $N_x\,a$, $N_y\,b$ and $N_z\,c$) affects the DP. Now for the next step, we will use this concept of the shape factor to examine how the DPs will be affected by more complex shapes, such as the wedge shape of many real TEM specimens or the perfect parallelepiped of the stacking fault. Then we will consider defects which themselves do not have sharp boundaries; the dislocation is a perfect example of such an imperfection.

17.3 DIFFRACTION FROM WEDGE-SHAPED SPECIMENS

Most TEM specimens do not have parallel surfaces but are wedge-shaped. In drawing the relrods for such a wedge-shaped specimen, we extend the results of Section 17.2

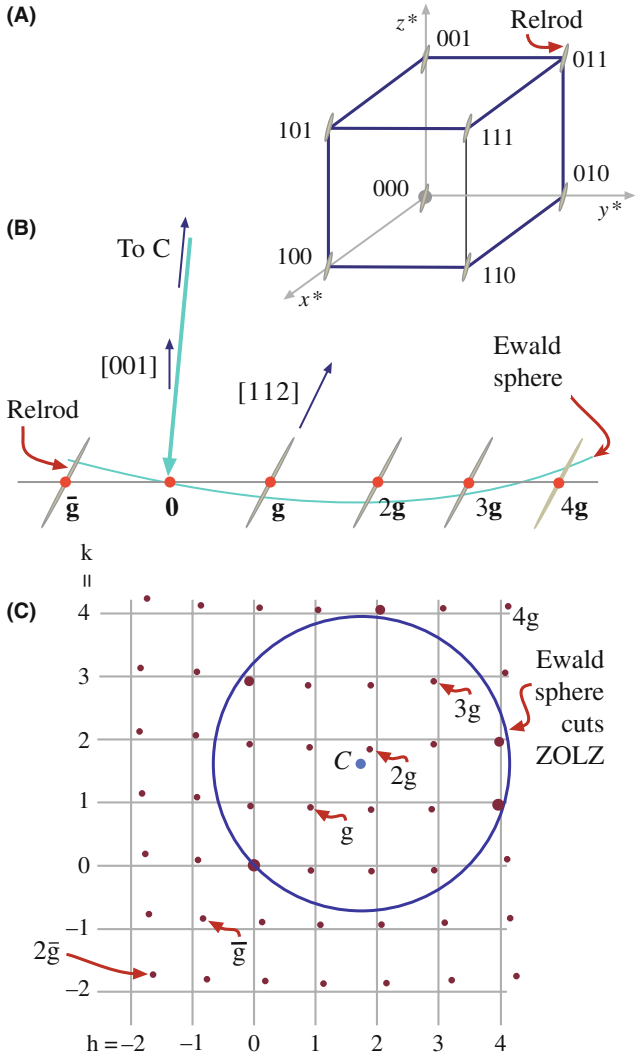

FIGURE 17.3. (A) For a thin specimen, every point is replaced by a relrod. (B) The Ewald sphere cutting the relrods in (A) when the crystal is tilted slightly off the (001) axis. (C) The effect of the tilt in (B) on the DP. Notice that all of the spots in the DP are displaced relative to their positions on the square grid (the projection of the spots at zero tilt), but that the magnitude of the displacement varies depending on the sign and size of **s**. Of course, spots on the Ewald sphere must be the 'correct' distance from 000.

by saying that the relrod will always be normal to the surface. So, for a wedge-shaped specimen (Figure 17.4A) we must have two relrods as shown in Figure 17.4B. What we see in the DP is determined by how the Ewald sphere cuts these two relrods. As shown in Figure 17.4C and D, we will see two spots which lie along a line which is normal to the edge of the wedge. Notice that all the pairs of spots are aligned in the same direction as we expected and that their separation is larger for larger values of **s**. This simple relrod model predicts that we would see only one spot if $\mathbf{s} = 0$. In fact, we should see two or more spots because the relrod model fails when we are in a strongly dynamical diffraction condition. We will return to this point in the next section and again in Chapter 24.

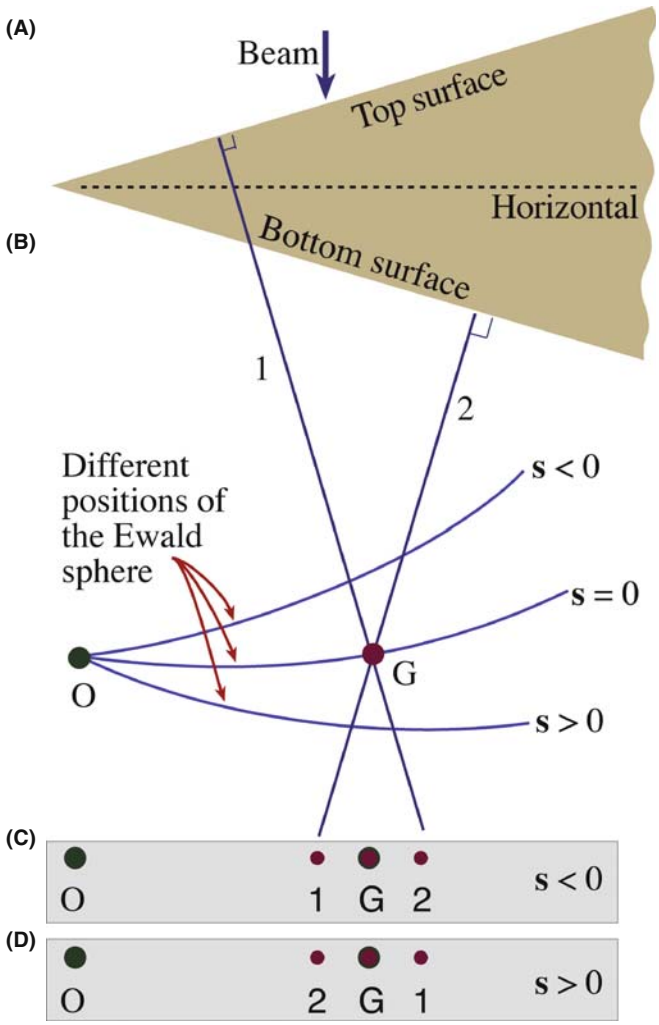

FIGURE 17.4. (A) Diffraction from a wedge-shaped crystal. (B) Notice that when $\mathbf{s} < 0$, relrod 1 is on the left of relrod 2 but the order reverses when $\mathbf{s}$ becomes > 0. The effect of this pair of relrods is to create a doublet shown in (C) and (D). The middle spot is the matrix relrod for a parallel-sided thin foil and is absent for the wedge in A.

17.4 DIFFRACTION FROM PLANAR DEFECTS

The shape factor concept can be readily applied to understand diffraction from a flat platelet or planar fault. The geometry is shown in Figure 17.5. The idea is that the platelet is itself a thin parallelepiped which is inclined to the specimen parallelepiped (Figure 17.5A). The result is that we have two relrods, one normal to the specimen surface and a much longer one normal to the thin platelet (Figure 17.5B and C). When we cut these relrods with the Ewald sphere we produce two spots in the DP and, as for the wedge specimen, the separation of the spots increases with increasing $\mathbf{s}$. The line MN lies normal to the trace of the platelet. There are, however, some differences in this case. Although the *m* and *n* relrods are very different in length and actual intensity,

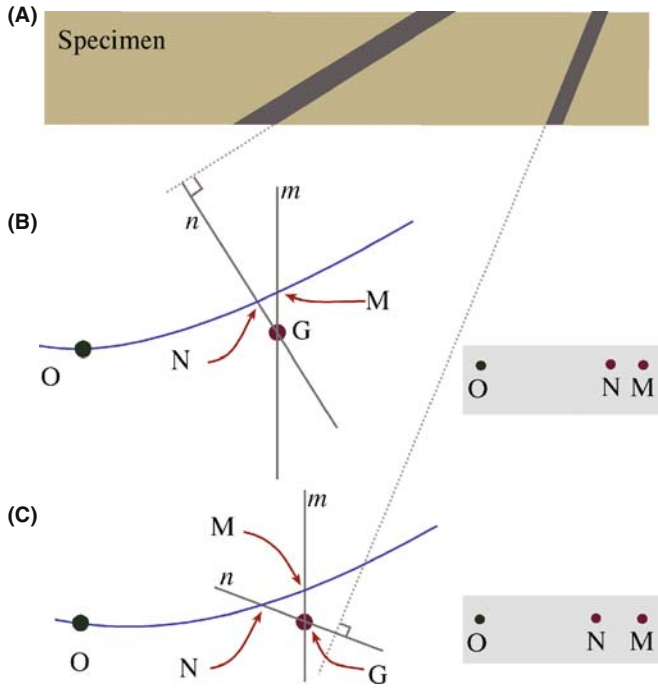

FIGURE 17.5. The effect of a thin inclined plate in a thin specimen. (A) Two plates are shown to illustrate the effect of changing the inclination of the plate relative to the foil surface. When $\mathbf{s} \neq 0$ we see two spots in the DP because there are two relrods for the two different planar-defect inclinations in (B) and (C).

the diffracting volume is much greater for the specimen than for the platelet. Thus, we can usually distinguish reflections M and N.

Providing we know the orientation of the specimen relative to the DP, we can tell whether the inclination angle is less than or greater than 90°; i.e., we can determine the inclination of the planar defect without moving the specimen or using any theory of image contrast (see Chapter 24). As in Section17.3, we would actually see two spots when $\mathbf{s} = 0$ if we could make the spots small enough. We'll return to this topic in Section 17.7.

A stacking fault in an fcc crystal can be thought of as a very thin platelet of hcp material as shown in Figure 17.6; so it really is a platelet with perfect lattice matching parallel to its surface.

We can understand diffraction effects from other planar interfaces by considering two cases

- If the grains on either side of the interface contain a common reflection, then the diffraction effects can be modeled by the thin platelet.
- In the case where a reflection is not common to the two grains, then for that reflection the diffracting crystal behaves like a wedge specimen with one surface parallel to the planar defect. We can ignore the crystal that is not diffracting.

The two DPs in Figure 17.7 show that you really do see pairs of spots for these two types of boundary. As

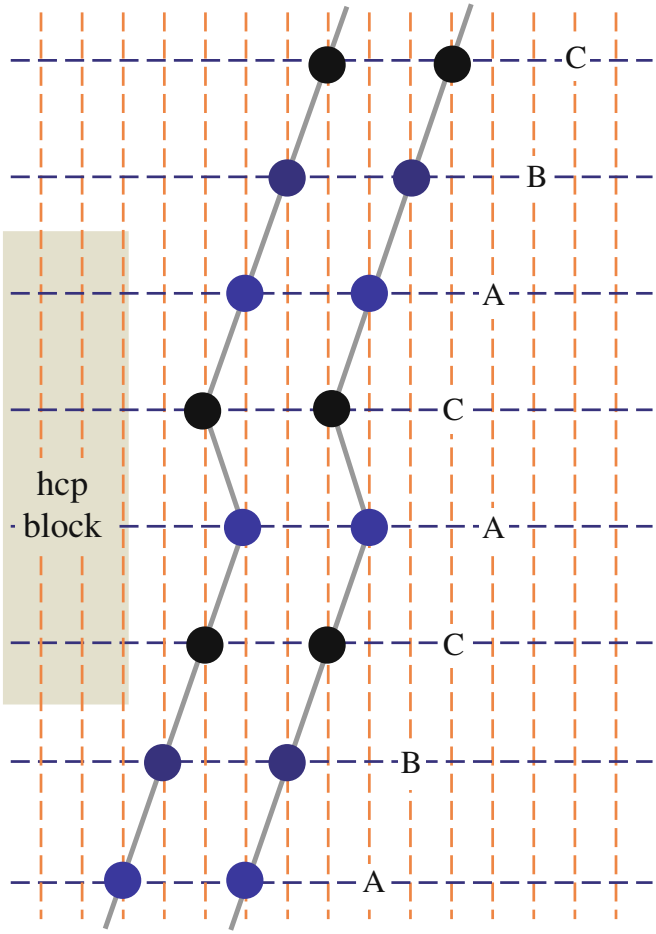

FIGURE 17.6. Schematic of the stacking sequence of close-packed planes A, B, C, in an fcc crystal showing that the SF is similar to a thin layer of hcp material, stacking ACAC.

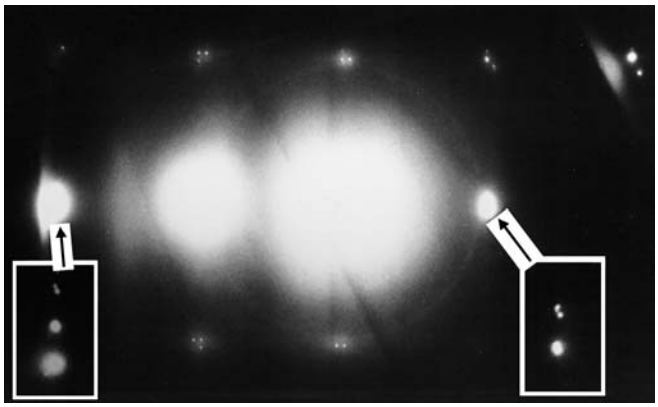

FIGURE 17.7. Pairs of spots in a DP from a grain boundary.

before, the two spots lie normal to the boundary traces, i.e., the intersection of the boundary with the surface of the specimen.

There are two reasons for emphasizing the extra spots which are present because of the interface

- You should always check that any extra spots you see cannot be explained in this way.
- You must be careful when determining spot spacing (as when estimating lattice parameters). You must set **s** to zero for this purpose and that can usually only be done for a few reflections at any time (one reflection always being O, not D, of course).

Twin boundaries are often found to consist of flat segments in particular orientations. The first-order twin boundary in fcc crystals tends to facet parallel to the common {111} plane as shown schematically in Figure 17.8A. This means that if we orient the specimen so that this common plane is nearly parallel to the beam, we will excite the common {111} reflection. Now our platelet is parallel to the beam so that its relrod is normal to the beam. If the specimen is also thin, we can arrange that the Ewald sphere cuts along the length of the relrod. Now, as we can see in Figure 17.8B, we see a 'streak' in the DP rather than a spot. The streak actually extends from in the [111] direction because, as you can appreciate from Figure 17.8A, the twin is a *very* thin platelet.

FROM NANOPARTICLES

Since we'll only detect any effect when the particle is $\leq$100 nm, these particles could be called nanoparticles. Anyone working with such particles must understand this effect which is closely related to Debye-Scherrer analysis in XRD.

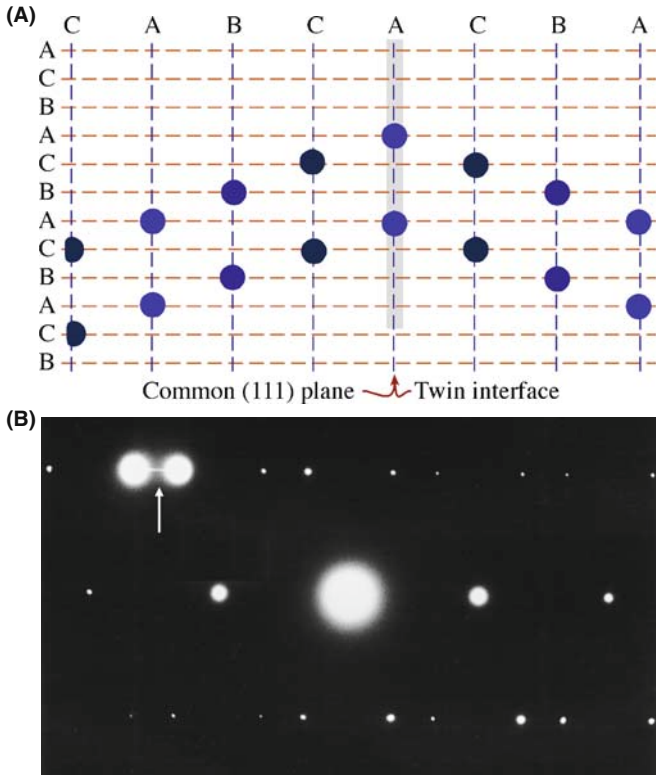

FIGURE 17.8. (A) Schematic of twin and (B) DP with a streak (arrowed) normal to the twin plane. Note that $\mathbf{s} = 0$ for the two bright diffracted spots.

If we regard the surface as a planar defect, we can also observe extra spots in the DP due to a reconstruction of the surface. One factor to be cautious about is that the apparent reconstruction might be influenced by contamination since the TEM is not generally a UHV system.

17.5 DIFFRACTION FROM PARTICLES

Particles come in all shapes and sizes, so we will not try to be exhaustive. Actually, the principle involved in determining the shape factor in reciprocal space is simply 'small becomes large' and vice versa. The shape factors are shown schematically for several particles in Figure 17.9. You should be aware that you will probably never see the subsidiary minima shown in these diagrams.

One example which is common is the platelet shown in Figure 17.10; these can occur as GP zones or other

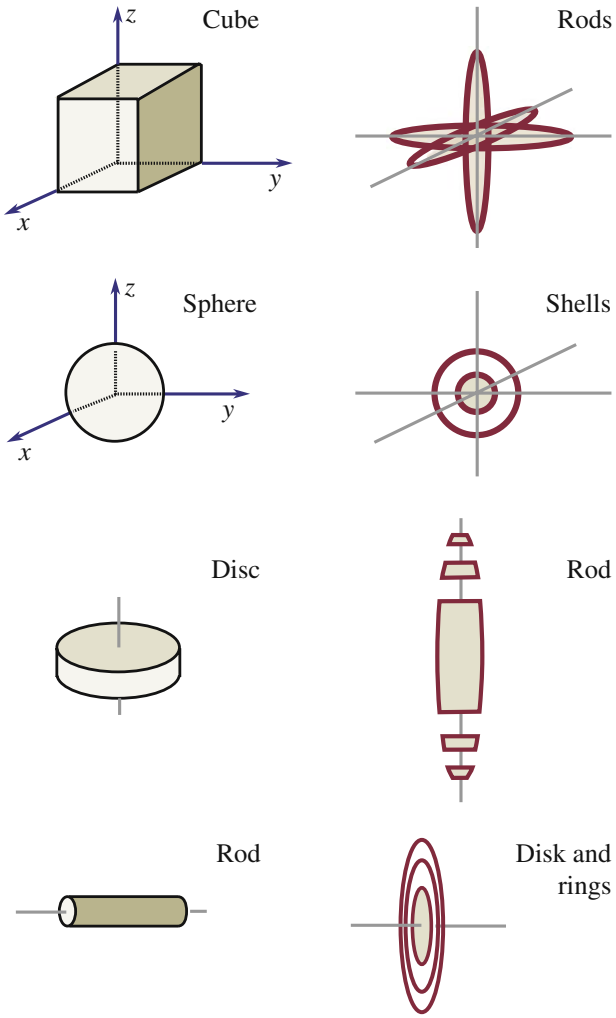

FIGURE 17.9. Examples of how spots in reciprocal space have different shapes depending on the shape of the particles which are diffracting.

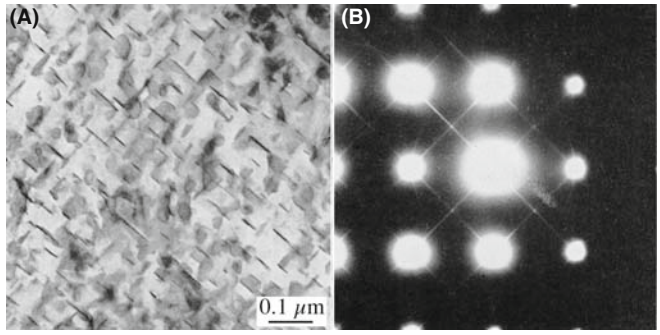

FIGURE 17.10. Very thin plate-like precipitates (A) cause long streaks in the DP (B). In this example, the precipitates are GP zones in an Fe-2.9 at.% Mo alloy.

thin disk-shaped precipitates. When the platelets are oriented parallel to the beam, we see streaks in the DP just as we saw them in Figure 17.8B. The difference in this figure is that the platelets can lie on all the crystallographically equivalent planes in the crystal. For these GP zones they lie on {001} planes so the streaks run in <001= directions for the cubic crystal connecting, for example, 000 and 200. You should notice that these spots would still be connected if the crystal were not cubic. You'll also see that there is a sharp point at the 100 position even though 100 is not an allowed reflection for bcc crystals. The reason we see this spot is that we are cutting the relrod which runs parallel to the electron beam in the [001] direction.

The smallest 'particle' can be thought of as a vacancy, a substitutional atom or an interstitial atom. We will not expect to see any clear effect of a single point defect but, as we saw in Section 16.7, these point defects can order to give a clear superlattice, and therefore extra spots.

As you might expect then, if we have many point defects but not enough to give long-range order, we might expect short-range ordering. Perhaps the clearest example of this phenomenon again occurs in the metal carbides. The effect is shown in Figure 17.11. The short-range ordering gives rise to diffuse scattering in the DP which at first appears quite random, sometimes as circles around the spots and appearing at other times as circles between spots or not circles at all! By combining many different patterns, Sauvage and Parthé proposed that the diffuse scattering could be mapped out as shown in Figure 17.11D. This figure strongly resembles a Fermi surface diagram which you may have encountered in condensed-matter physics. We will discuss some aspects of imaging using diffusely scattered electrons in Section 29.4, but the important points to recognize are

- Point defects really can cause diffraction effects, especially if they interact with one another.
- Diffuse scattering can still be interpreted by the Ewald-sphere construction.

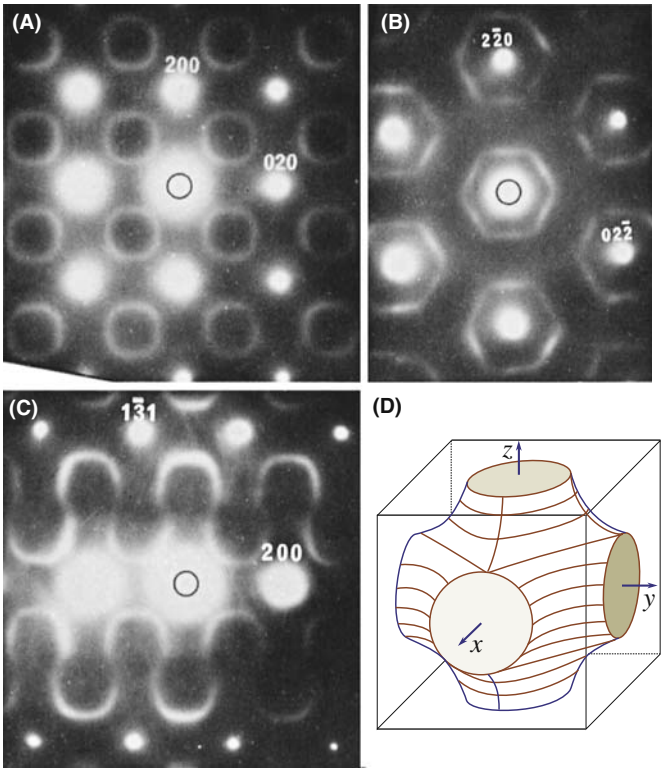

FIGURE 17.11. Short-range ordering can cause diffuse scattering in the DP (A–C). The DPs in this example were obtained from a vanadium carbide. In this case, the 3D map of diffuse intensity has a shape which strongly resembles a Fermi surface shown in (D).

If you are intrigued by this topic, you will find the literature on discommensurate structures in intercalated material a complementary challenge. A library/web search on 'discommensurate' and 'intercalated' will quickly net more recent papers.

17.6 DIFFRACTION FROM DISLOCATIONS, INDIVIDUALLY AND COLLECTIVELY

In Chapter 25 we will discuss images of dislocations. A dislocation is a line defect that is characterized by its line direction and its Burgers vector. The crystal around the defect is distorted or strained.

For a single dislocation, this strain is not expected to cause new spots in the DP, but we do expect diffuse scattering since the dislocation is a line defect. If a region from 0.2 to 1 nm around the core is greatly distorted (we'll see the effect of this strain in Chapter 25), then the diffuse scattering will extend from 1 nm^{-1} to perhaps 5 nm^{-1} from the reciprocal-lattice points, giving a diffuse disk (the reciprocal shape of a long needle). Some planes are essentially unaffected by the dislocations, so we might expect the diffuse scattering to vary in magnitude for the different reciprocal-lattice points. (We'll examine this $\mathbf{g}.\mathbf{b} = 0$ effect in Chapter 24.)

With this simple discussion and without ever seeing this diffuse scattering, we can draw an important conclusion: if we want to learn about the structure of a dislocation core, we must include the diffuse scattering in the image-formation process. We must include that intensity in the objective aperture and the corresponding image calculations.

DIFFUSE SCATTERING
The diffuse intensity from a dislocation is *not* located at the reciprocal-lattice point.

Because the distorted volume associated with a single dislocation is so small, we do not expect to see this intensity in the DP unless we have many dislocations in an ordered array (just like the point defects in Section 17.5). We can demonstrate that this intensity is present by diffracting from an ordered array of dislocations as shown in Figure 17.12. The specimen used to form this image was rather special. Dislocations are present in region A, but not in region B. The array actually forms a structured grain boundary in A, but a layer of glass is present in B. The insets show the same part of the SADPs from the two regions. In B, you can see three spots. The top two are from one grain, the bottom one is from the other grain. The reason for the pair is that **s** is

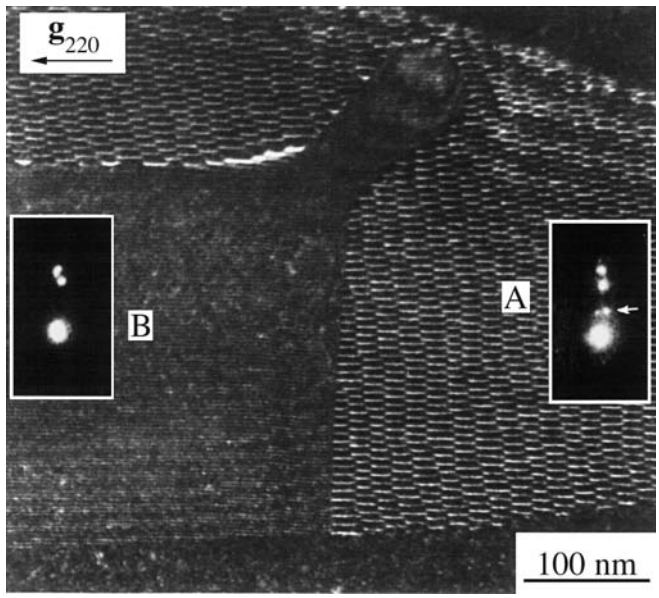

FIGURE 17.12. Diffraction from an ordered array of dislocations. Dislocations are present in region A, but not in region B. The insets show a small part of the DP from the two regions. The extra spots present in A are caused by the visible array of dislocations; these spots are a doublet because there is also a second, nearly orthogonal, set of dislocations present which acts as a separate grating. The other pair is due to the wedge shape and so is common to both DPs.

large for that grain, but almost zero for the other. This is an example of the application of Section 17.3.

In A you see the same three spots (because the two grains are still present) but now there are two extra spots. The reason we see two extra spots is that we have two arrays of dislocations. You are seeing the scattering from the dislocations because they have formed an array with long-range ordering, just like the vacancies in V_8C_7 in Chapter 16.

If you look at the DP when the array of dislocations lies parallel to the beam, you may be able to see a set of streaks as shown in Figure 17.13. The separation of the streaks is the inverse of the actual separation of the dislocations. You see streaks because you have relrods in reciprocal space and we are cutting along these rods with the Ewald sphere. The length of the relrods gives you a measure of how far the strain field of the dislocations extends out into the two grains. In other words, we are seeing a thickness of the strain-field regions. The object of this discussion is not to examine grain boundaries, but to show that the strain field from an array of dislocations causes scattering in the DP and thus to infer that one dislocation will also cause scattering, but it will just be much more diffuse (and very weak).

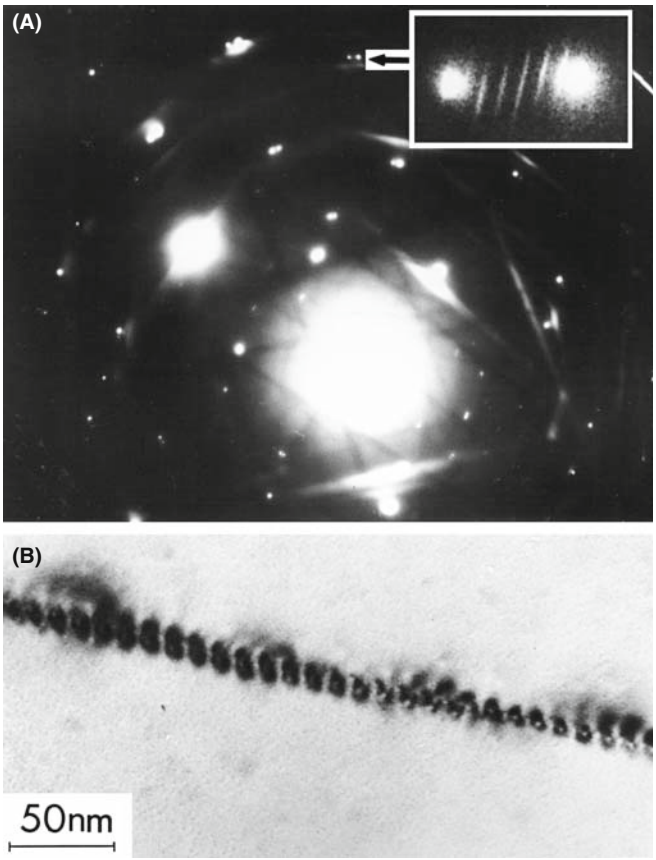

FIGURE 17.13. (A) The set of streaks from an array of dislocations in Al_2O_3 lying parallel to the electron beam. The distance between the streaks is inversely related to the spacing of the dislocations shown in the image (B).

Before moving on, consider the diffraction spots in Figure 17.12 again. Why are the pairs of dislocation spots (arrowed) located where they are? Put another way: which of the two spots in region B corresponds to the N relrod and which corresponds to the M relrod? (See Figure 17.5 for the definition of M and N.)

THE PERIODICITY RULE

If there is a structural periodicity in real space, then there will be an array of points or relrods in reciprocal space and an array of spots or streaks in the DP.

We then ask a simple question: how many objects are required in order to produce a detectable effect in the DP? The answer is two! This point is illustrated in Figure 17.14, which shows a DP and an image of two twin boundaries which are ~15 nm apart. The spacing of the new spots between the twin spots in the DP (expanded in the inserts) is 0.067 nm^{-1}, as expected. Now, why can this occur? The analogy is the Young's slits experiment in visible-light optics. The illustration also reminds us of a special feature of the TEM, namely, that even without a FEG, the electron beam is remarkably coherent.

17.7 DIFFRACTION AND THE DISPERSION SURFACE

Several times in this chapter, we have said "actually, we will see two spots when $\mathbf{s} = 0$," even though the relrod model says that you will only see one. The origin of two spots from a wedge specimen (there may be more for more complicated defects) is due to the dynamical nature of the scattering process. The theory has been derived by Amelinckx and his co-workers in a series of papers. Unfortunately, this group used a different notation, but they did summarize their results graphically. We will also return to this topic when we discuss images in Chapter 24. As an example, the relrod diagram given for the stacking fault in Figure 17.5 should be drawn so that the relrods are the asymptotic to two straight lines, as shown in Figure 17.15. When the Ewald sphere cuts these curves at $\mathbf{s} = 0$, we see that there are two spots which move apart as we increase $\mathbf{s}$ (either positive or, as shown here, negative) until they are at the points defined by the straight lines. So, will there not be a vector that exactly corresponds to $\mathbf{g}$? The answer, of course, is yes, because of the adjacent perfect crystal so we must have three spots, but these are very difficult to see because $\mathbf{s}$ must be very close to zero. Without going into any theory, we can guess the origin of these curves: they look remarkably like the curves of the dispersion

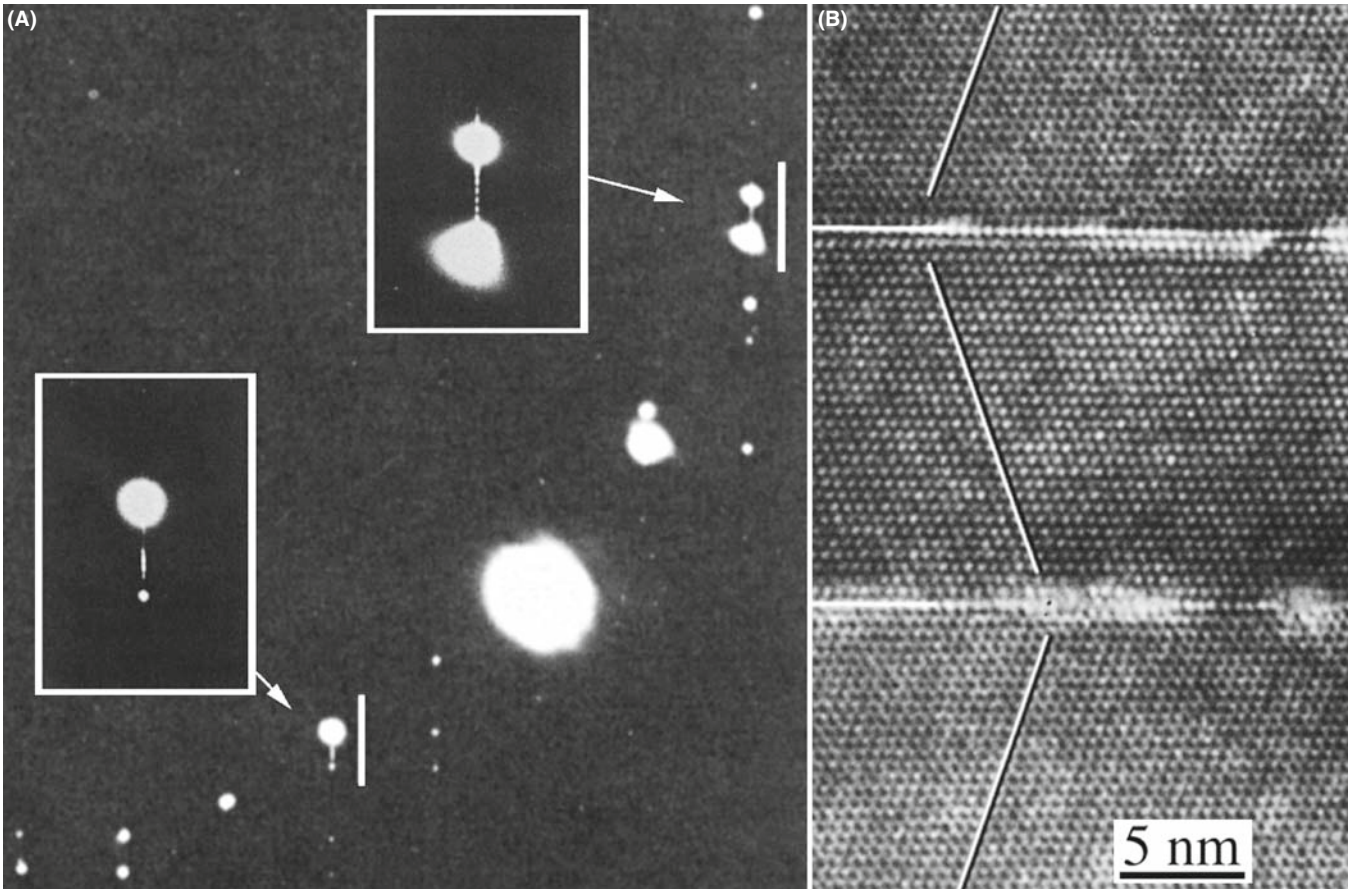

FIGURE 17.14. Extra spots can be formed in the DP (A) when only two defects are scattering in phase. The separation of the extra spots is related to the inverse of the separation of the two twin boundaries seen in the image (B).

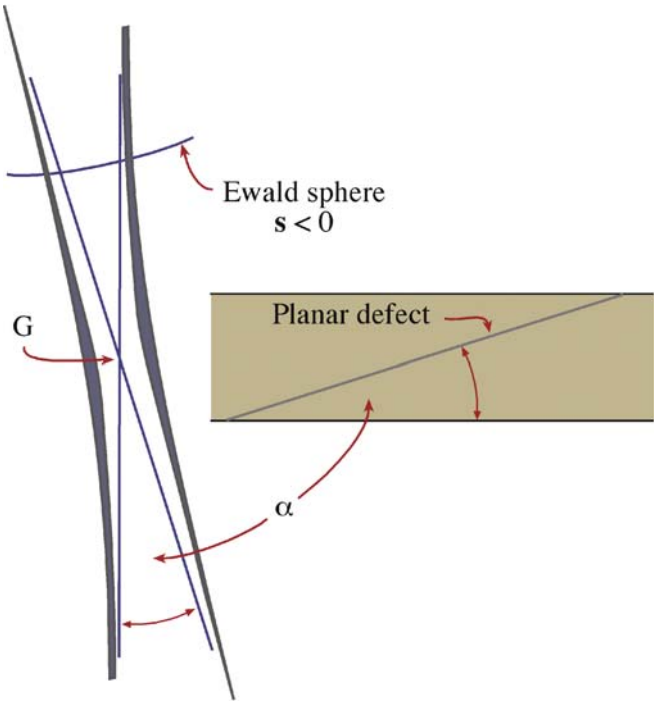

FIGURE 17.15. The relrods from two planes inclined at angle α are actually the asymptotes to two straight lines, so that they don't cross at G; when $\mathbf{s} = 0$, the distance between these two curves is $\xi_{\mathbf{g}}^{-1}$.

surface which also had asymptotes (see Figure 15.3). These curves are indeed directly related.

When you increase **s,** you move out of the dynamical regime and into the kinematical one, where the simple relrod model applies (see Chapter 26). At $\mathbf{s} = 0$, the distance between the curves is inversely proportional to $\xi_{\mathbf{g}}$, the extinction distance for reflection **g**.

You can understand why this is so in the following pictorial way. What you see in the image will be determined by the DP. What you see in the DP is determined by which relrods, or surfaces, the Ewald sphere intersects. All the information about extinction distances and coupling of diffracted beams is fundamentally contained in the dispersion surface ($\xi_{\mathbf{g}}$ is just Δk^{-1} at $\mathbf{s} = 0$). Both the dispersion surface and the reciprocal-lattice/Ewald-sphere models are just pictorial representations of the same diffraction process. So, all the information in the dispersion-surface model should also be present in the reciprocal-lattice/Ewald-sphere model.

The relrods are the asymptotes to these two hyperbolas. Alternatively, we could say that the relrods and the asymptotes are a result of the kinematical diffraction

approximation. There is a one-to-one correlation between what happens at the dispersion surface in the vicinity of the BZB to what happens when the Ewald sphere cuts the relrods in the vicinity of the reciprocal-lattice point, G. Imagine rotating the dispersion-surface diagram through 90°. These ideas have been extensively studied by van Landuyt, de Ridder, Gevers, Amelinckx et al., as summarized in the general references at the end of this chapter. What Amelinckx's group has done is to give us the rules on how to transfer this information from the dispersion surface to the reciprocal lattice and hence to the DP. In Section 24.9, we'll relate this concept to images. If you thought dispersion surfaces were difficult, make **s** large and stick to relrods!

CHAPTER SUMMARY

In this chapter, we have begun to examine the unique features of diffraction in the TEM. These features arise because we are always diffracting from small volumes. The sizes of both our specimen and the special features present in our specimen are always small, so that we must take into account the shape effect. This is particularly important for nanoparticles and nanograins—you must keep this in mind when imaging. Of course, the same considerations will also apply to other forms of diffraction; it's just that only TEM can examine the diffraction information from the vicinity of crystal defects. In other words, the shape effect is not a limitation due to the fact that we are using high-energy electrons. By understanding the concept of the shape effect you can actually learn more about defects in crystals; conversely, you can make some major errors if you do not understand the shape effect. Two points to remember are

- When a platelet is parallel to the beam its relrod is normal to the beam. If the specimen is also thin, we can arrange that the Ewald sphere cuts along the length of the relrod. Now you see a 'streak' in the DP rather than a spot.
- Beam splitting at $\mathbf{s} = 0$ and the dispersion surface both arise because of dynamical scattering.

DIFFRACTION FROM INTERFACES

The relation between diffraction and images from planar defects has been the subject of a long series of papers from the group led by Prof. Severin Amelinckx. The examples below from Phys. stat. sol. will give you a start to your study.

Carter, CB (1984) *Electron Diffraction from Microtwins and Long-Period Polytypes* Phil. Mag. A **50** 133–141. The Young's slit experiment in the TEM.

de Ridder, R, Van Landuyt, J, Gevers, R and Amelinckx, S (1968) *The Fine Structure of Spots in Electron Diffraction Resulting from the Presence of Planar Interfaces and Dislocations. IV. Wedge Crystals* Phys. stat. sol. **30** 797–815; See also: (1970) *ibid.* **38** 747; (1970) *ibid.* **40** 271; (1970) *ibid.* **41** 519; (1970) *ibid.* **42** 645.

Gevers, R (1971) in *Electron Microscopy in Materials Science* (Ed. U. Valdrè) p302–310, Academic Press, New York. An introduction to the work of Amelinckx' group.

Gevers, R, Van Landuyt, J and Amelinckx, S (1966) *The Fine Structure of Spots in Electron Diffraction Resulting from the Presence of Planar Interfaces and Dislocations. I. General Theory and Its Application to Stacking Faults and Anti-phase Boundaries* Phys. stat. sol. **18** 343–361; See also (1967) *ibid.* **21** 393; (1967) *ibid.* **23** 549; (1968) *ibid.* **26** 577.

Van Landuyt, J (1964) *An Electron Microscopic Investigation of Phenomena Associated with Solid Solution of Oxygen in Niobium* Phys. stat. sol. **6** 957–974.

Van Landuyt, J, Gevers, R and Amelinckx, S (1966) *On the Determination of the Nature of Stacking Faults in fcc Metals from the Bright Field Image* Phys. stat. sol. **18** 167–172.

DIFFUSE SCATTERING AND INTERCALATION

Carter, CB and Williams, PM, 1972, *An Electron Microscopy Study of Intercalation in Transition Metal Dichalcogenides* Phil. Mag. **26** (2), 393–398. To encourage new students!

Sauvage, M and Parthé, E (1972) *Vacancy Short-Range Order in Substoichiometric Transition Metal Carbides and Nitrides with the NaCl structure. II. Numerical Calculation of Vacancy Arrangement* Acta Cryst. **A28** 607–616.

Wilson, JA, Di Salvo, FJ and Mahajan, S (1975) *Charge-Density Waves and Superlattices in the Metallic Layered Transition Metal Dichalcogenides* Adv. Phys. **24** 117–201. An early review of intercalation.

THE COMPANION TEXT

Although there is great interest in nanomaterials and XRD is often used to characterize them, diffraction from such materials in the TEM is used much less because imaging is then almost routine. Hence there have not been recent advances in electron diffraction except as CBED, which is treated in the companion text.

SELF-ASSESSMENT QUESTIONS

Q17.1 When the Bragg condition is not satisfied exactly, why do spots appear in the DP?
Q17.2 Reproduce the summation and integral calculations of amplitudes to explain the existence of relrods.
Q17.3 When the specimen is tilted slightly off a particular zone, why might spots in the DP move away from their ideal positions in the DP?
Q17.4 Is a relrod a 'real' object?
Q17.5 In a specimen containing thin platelets, how is it possible to distinguish the DP spots associated with the thinness of the specimen from those due to the platelets?
Q17.6 If a single dislocation is observed in the specimen, should the DP change?
Q17.7 When is it possible to view along the entire length of a relrod?
Q17.8 The spots in the right inset of Figure 17.14 are very clear. Why did we show this region rather than the region between 000 and the common 111?
Q17.9 What is the definition of a twin boundary?
Q17.10 For what conditions might you see diffuse circles surround the DP spots?
Q17.11 How does the thickness of the TEM foil affect how (when) the Laue conditions are satisfied?
Q17.12 How can the thickness of the specimen affect the accuracy of lattice-parameter determination?
Q17.13 How can the wedge shape of a specimen influence the appearance of the diffraction spots?
Q17.14 When $\mathbf{s} = 0$, the (curved) relrod models predicts two spots will be seen in the DP. Why?
Q17.15 In Figure 17.8, we can see a streak between two spots in the DP. What does this tell us?
Q17.16 It is only possible to see a streak in the DP when the specimen is thin. Explain.
Q17.17 Does short-range ordering give rise to effects in the DP?
Q17.18 In Figure 17.5, what determines the distance between spots M and N?
Q17.19 When viewing a twist boundary nearly flat on, we look at the DP and see that there are three spots at $-2\mathbf{g}$ and two spots at $+\mathbf{g}$? Why is there an extra spot at $-2\mathbf{g}$?
Q17.20 Why is the $2\mathbf{g}$ reflection inside the square but $4\mathbf{g}$ reflection outside for the DP in Figure 17.3C?
Q17.21 For a wedge specimen, we say we have two sets of relrods because there are two surfaces. How does this fit with our idea of relrods arising from thin plates?
Q17.22 Can you see an effect in the DP if a twin boundary is viewed flat on?
Q17.23 Why do we see the (100) reflection in Figure 17.10?
Q17.24 How many objects are required in order to produce a detectable periodicity in the DP?

TEXT-SPECIFIC QUESTIONS

T17.1 Consider Figure 17.13 and the relationship of streak length to defect (interface) width. What is the width of the grain boundary according to the DP?
T17.2 Examine the extra spots in inset A of Figure 17.12. Compare the spacing of dislocations giving rise to these spots with the periodicity of the spots.
T17.3 Explain why there are spots in inset B of Figure 17.12.
T17.4 Consider Figure 17.15. How would this figure change if the top half of the figure (above the planar defect) were removed?
T17.5 Consider Figure 17.14B. Construct the DP you expect to see, assuming it's Si.
T17.6 Consider Figure 17.7. If this DP is from an 001 twist boundary, what is the angle of misorientation?
T17.7 Consider Figure 17.7. How can the lower reflection be the brighter in both insets?
T17.8 Consider Figure 17.3. Redraw the figure with the Ewald sphere cutting through (−2, −2) and (0, −2).
T17.9 Fully index the DP in Figure 17.10. Explain why this material must be BCC and not FCC.
T17.10 Why is the streak seen where it is in Figure 17.8?
T17.11 Figure 17.8A shows two grains. Which spots in Figure 17.8B correspond to which grains?
T17.12 Look at Figure 17.14. Is the spacing of the fine spots in the inset consistent with the image? Justify your answer.
T17.13 Consider Figure 17.14. Why are there several spots in a row rather than just one extra spot?
T17.14 Why do the streaks in Figure 17.13 shift parallel to their length as we look from one spot to the other in the insert?
T17.15 A thin Al metal foil contains needle-shaped precipitates which are 2 nm in diameter and 20 nm long. The needle lies in the (001) plane and its axis is parallel to the [110] direction. Sketch the [001] DP of the foil. (Courtesy ZL Wang.)